

FUZZY SELECTING LOCAL REGION LEVEL SET ALGORITHM

Souleymane BALLA-ARABE, Chao LI, Vincent BROST, Fan YANG

LE2I CNRS 6306, University of Burgundy

ABSTRACT

In this work, we introduced a novel localized region based level set model which is simultaneously effective for heterogeneous object or/and background and robust against noise. As such, we propose to minimize an energy functional based on a selective local average, i.e., when computing the local average, instead to use the intensity of all the pixels surrounding a given pixel, we first give a local Gaussian fuzzy membership to be a background or an object pixel to each of these surrounding pixels and then, we use the fuzzy weighted local average of these pixels to replace the traditional local average. With the graphics processing units' acceleration, the local lattice Boltzmann method is used to solve the proposed level set equation. The algorithm is effective in presence of intensity heterogeneity, robust against noise, fast and highly parallelizable. Experimental results demonstrate subjectively and objectively the performance of the proposed framework.

Index Terms—Level set method, image segmentation, lattice Boltzmann method, graphics processing units (GPU)

1. INTRODUCTION

The level set method (LSM) [1] refers to the geometric representation of active contours models [2]. It is a numerical technique for tracking interfaces and shapes. In recent years, it has attracted much more attention due to its advantageous qualities which allow to easily handle complex shapes and topological changes. In two-dimensional (2D) space, the LSM represents a closed curve in the plane as the zero level set of a three-dimensional (3D) function ϕ . The curve has to move toward its interior or exterior normal until defining the boundary of the object of interest. The active contour evolution is driven by the level set equation (LSE) which is a partial differential equation and, in its general form can be expressed as

$$\partial\phi/\partial t = |\nabla\phi|(\alpha V + \beta\nabla\cdot(\nabla\phi/|\nabla\phi|)), \quad (1)$$

where ϕ is the level set function (LSF), V is the speed function which drives the active contour towards the region boundaries, the second term in the brackets of the right hand represents the curvature and is used to smooth the contour, α and β are user-controlling parameters.

Generally two methods can be used to stop the evolving curve on the boundaries of the desired objects. The first one uses an edge indicator depending on the gradient of the image like in classical snakes and active contour models [3]; the second approach employs some regional statistics to stop the evolving curve [4]. The latter approach can detect objects which boundaries are not defined by clear edges and, comparing with the first one, it is more robust against noise since it uses regional information. The active contours without edges method of Chan and Vese [4] is one of the most widely used region-based LSM. In this model, the image is partitioned into two phases by the active contour; the means of the intensity values inside and outside the contours are then used to decide if a given pixel is inside wherever outside the contour. The method is robust against noise and effective in many cases, but it fails when the image presents intensity heterogeneity where the foreground and the background share nearly the same statistics. This limit is due to the use of the global intensity average inside and outside the contour, and many good solutions have been proposed for this problem, for example in [14] the authors propose to use local intensity average instead of the global one, in [15] the authors propose to minimize the sum of an edge-based energy and a region-based energy. But the use of local information increases the sensitivity to noise since the noise intensities can easily affect local average than global average.

In this paper, we propose a selective local region-based level set algorithm which has the advantage of local region method and is more robust against noise than global region methods. Our basic idea is when computing the local average, instead to use the intensity of all the pixels surrounding a given pixel, we first give a local Gaussian fuzzy membership to be a background or an object pixel to each of these surrounding pixels and then, we use the fuzzy weighted average of these pixels to replace the traditional local average that will be used to decide either that pixel is inside or outside the evolving curve. Since the method concedes small memberships values to noise and high membership's values to the background and the object pixels, the noise impact is quietly suppressed. Furthermore, we make the algorithm faster and suitable for parallel programming by using the lattice Boltzmann method (LBM) as an alternative approach to solve the LSE. The LBM is recently used in image segmentation [5], [9], [17] but highly promising because of its simplicity, explicit and highly parallelizable nature. It is second order accuracy both in time and space and can better handle the problem of time consuming because the non-linear term in

Thanks to the Regional Council of Burgundy for funding.

the LSE, i.e., the curvature term, is implicitly computed. The LBM is firstly designed to simulate Navier-Stokes equations for an incompressible fluid [6]. The evolution equation of LBM is

$$f_i(\vec{r} + \vec{e}_i, t+1) - f_i(\vec{r}, t) = \Omega_{coll}, \quad (2)$$

where f_i is the particle distribution function and Ω_{coll} is, in this paper, the Bhatnager-Gross-Krook (BGK) collision model [7], [18] with a body force \vec{F} .

$$\Omega_{coll} = (1/\tau)[f_i^{eq}(\vec{r}, t) - f_i(\vec{r}, t)] + (D/bc^2) \cdot \vec{F} \cdot \vec{e}_i, \quad (3)$$

where D is the grid dimension, b is the link at each grid point, c is the length of each link which is set to 1 in this paper, τ represents the relaxation time and f_i^{eq} the local Maxwell-Boltzmann equilibrium particle distribution function expressed in its continuous form as

$$f_i^{eq} = \rho(2\pi RT)^{-3/2} \exp[-(\vec{v} - \vec{u})^2 / 2RT], \quad (4)$$

where \vec{v} is the particle velocity and \vec{u} the macroscopic velocity. The equilibrium distribution can be expressed in discrete form as follows when modeling typical diffusion phenomenon,

$$f_i^{eq}(\rho) = \rho A_i \quad \text{with } \rho = \sum_i f_i, \quad (5)$$

where ρ is the macroscopic fluid density. By performing the Chapman-Enskog expansion [16] the following diffusion equation can be recovered from LBM [6],

$$\partial\rho/\partial t = \beta \text{div}(\nabla\rho) + F. \quad (6)$$

Substituting ρ by the signed distance function ϕ in Eq. (5), the LSE can be recovered. In our model we use the D2Q9 ($D=2, d=9$) LBM lattice structure. The body force F acts as the image data link for the LBM solver. Since the LBM is local and thus suitable for parallel programming, the proposed algorithm is accelerated using an NVIDIA GPU. The proposed method is robust against noise, fast and efficient when detecting objects for which boundaries are not clearly defined even in presence of serious intensity heterogeneity.

The remainder of this paper is organized as follows. Section II details the formulation of the proposed model. Experiments on various kinds of images are presented in Section III, whereas the conclusions are drawn in Section IV.

2. THE PROPOSED LEVEL SET MODEL

This section presents the proposed level set method based on selective local region and its implementation details. The energy functional to minimize is defined as

$$\mathcal{E}(\phi) = \mathcal{E}_{img}(\phi) + v_L \int_{\Omega} |\nabla H(\phi)| dx + v_A \int_{\Omega} H(\phi) dx, \quad (7)$$

With

$$\begin{aligned} \mathcal{E}_{img}(\phi) &= \alpha \int_{\Omega} (a_1(x) - I(x)) H\phi(x) dx \\ &\quad - \beta \int_{\Omega} (a_2(x) - I(x))(1 - H\phi(x)) dx \end{aligned} \quad (8)$$

s.t. $\alpha + \beta = 1$ with $\alpha > 0$ and $\beta > 0$.

The energy term $\mathcal{E}_{img}(\phi)$ is the link with image data. The second term at the right hand of Eq. (7) is the contour regularization term with v_L a positive coefficient, the third term is the constraint on the area inside the contour with v_A a positive coefficient, H is the Heaviside function, ϕ the level set function which is here a signed distance function, Ω is the computing domain. The terms $a_1(x)$ and $a_2(x)$ are the local selective intensity average respectively inside and outside the evolving contour, which are defined as

$$a_1(x) = \frac{\int_{\Omega} k(x, y) H\phi(y) H(\mu(y) - t) I(y) dy}{\int_{\Omega} k(x, y) H\phi(y) H(\mu(y) - t) dy}, \quad (9)$$

$$a_2(x) = \frac{\int_{\Omega} k(x, y) (1 - H\phi(y)) H(\mu(y) - t) I(y) dy}{\int_{\Omega} k(x, y) (1 - H\phi(y)) H(\mu(y) - t) dy}, \quad (10)$$

where $\mu(x)$ is the fuzzy membership of a given pixel x and t is a threshold value below which a pixel is consider to be a noise, thus its intensity is not used when computing $a_1(x)$ and $a_2(x)$. The membership matrix μ is defined as follows. Let consider the 2D gray-scale histogram of an $M \times N$ image as the set

$$H_{2D} = \{h_{ij} / h_{ij} = \text{number of bin}(i, j), 0 \leq h_{ij} \leq M \times N\}, \quad (11)$$

where element g_{ij} is the number of gray-scale bins with

$$(I, I_{mean}) = (X - \text{axis}, Y - \text{axis}), \quad (12)$$

where I_{mean} is gray level the local average. The straight line $I = I_{mean}$ in 2D gray-scale histogram represents more likely the objects and the background pixels. The more we go far from this line, the more likely the pixel represents noise or edges. We can thus represent the fuzzy membership of a given pixel to belong to the objects or the background (and not to be a noise or an edge) by Gaussian membership function centered at I_{mean} . For a given pixel x , $\mu(x)$ is then expressed as

$$\begin{aligned} \mu(x) &= \exp\left\{-(1/2s)|I(x) - I_{mean}(x)|^m\right\} \\ \text{with } I_{mean}(x) &= \frac{\int_{\Omega} k(x, y) I(y) dy}{\int_{\Omega} k(x, y) dy}, \quad k(x, y) = \begin{cases} 1, & |x - y| < r \\ 0, & \text{otherwise} \end{cases} \end{aligned} \quad (13)$$

where x and y are spatial variables, r a radius constant, s the width and m the fuzzification factor. Fig. 1 shows the fuzzy membership matrix μ of a given image. From Fig. 1, we can see as expected that the background and the object have the membership value equal to one (white pixels) and the edges have the lower membership value.

By using the gradient descent method

$$\partial\phi/\partial t = -\partial\mathcal{E}/\partial\phi, \quad (14)$$

where $\partial\mathcal{E}/\partial\phi$ is the Gâteaux derivative [8] of \mathcal{E} , we obtain the following level set equation

$$\begin{aligned} \partial\phi/\partial t = & (I(x) - (\alpha a_1(x) + \beta a_2(x)) \\ & + v_L \operatorname{div}(\nabla\phi/|\nabla\phi|) - v_A) \cdot \delta(\phi). \end{aligned} \quad (15)$$

Considering the above defined LSE, the gradient projection method [10] allows us to replace $\delta(\phi)$ by $|\nabla\phi|$, and as ϕ is a signed distance function we have $|\nabla\phi|=1$. The equation can therefore be simplified as follows,

$$\partial\phi/\partial t = v_L \operatorname{div}(\nabla\phi) - v_A + I(x) - (\alpha a_1(x) + \beta a_2(x)), \quad (16)$$

which is similar to Eq. (6) with the body force expressed as

$$F = -v + \lambda(I(x) - (\alpha a_1(x) + \beta a_2(x))), \quad (17)$$

where v and λ are positive parameters. The proposed level set equation can therefore be solved using LBM with the above defined body force, without the necessity of explicitly compute the curvature since it is implicitly handled.

3. EXPERIMENTAL RESULTS AND ANALYSIS

In this section, we carried out several experiments using various kinds of images in order to demonstrate the performance of the proposed method. We compared subjectively and objectively the method, in terms of efficiency, speed and effectiveness, with three level set methods. The first one is an edge-based method proposed by Li *et al.* in [11] where the main idea was to perform a level set segmentation without re-initialization. The second method is the well-known global region-based level set segmentation method proposed by Chan and Vese (C-V) in [4]. It is robust against noise but can easily be trapped into local minima and is not ideal for image segmentation in

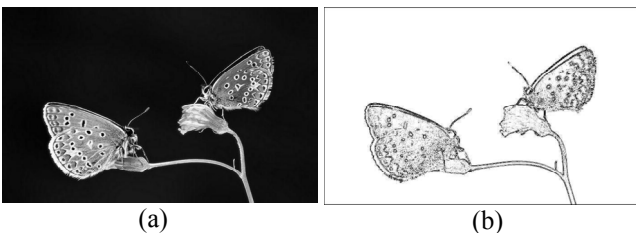


Fig. 1. (a) Original image, (b) the corresponding local Gaussian membership matrix μ with $s = 2$.

presence of intensity heterogeneity. The third one is a lattice Boltzmann based method proposed by Chen *et al.* in method [5] where the authors considered a medium between the nodes of the lattice, the particles can pass through the medium if the local gradient value is small and will be punched back if the value is high.

The objective evaluation is done by mean of the Levine and Nazif (LN) inter-region and intra-region contrast criterion [12]-[13]. The lower is the intra-region contrast, the better is segmentation result, and the higher is the inter-region contrast, the better is the segmentation result.

The GPU implementation have been done using the parallel computing toolbox of Matlab R2012a installed on a PC AMD Athlon (TM) 5200 processor with a clock speed of 2.31 GHz, 2 GB of RAM and possessing the NVIDIA GPU GT 430. When measuring the executive time, we subtract the CPU-GPU and GPU-CPU data transferring time. We fixed the fuzzification parameter $m = 2$, the thresholding parameter $t = 0.85$, the width of the Gaussian membership function $s = 2$, the radius constant $r = 2$, the parameter $\lambda = 10$, the positive constants $v = 2$, $\alpha = 0.5$ and $\beta = 0.5$. We implemented the body force and only the collision step on GPU, since this step is fully local the speed up is considerable, the streaming step is executed on the CPU. The optimized Matlab function *arrayfun* is used to execute the code on the GPU. For example, the following code is used to compute the body force.

The two first instructions transfer respectively I and I_{mean} from the CPU to the GPU. The third instruction computes the body force on the GPU using the kernel function *Gauss_Body_force.m* programmed according to Eq. (17). The Fourth instruction transfers the computed body force F from the GPU to the CPU.

In order to better allow the subjective evaluation, we presented some results in two forms, being contour and binary representations. To obtain the binary representation, the interior of the final LSF is represented by white pixels and the exterior by black pixels.

Fig. 2 shows the performance on a natural image, the executive times and the results of the objective evaluation are displayed by TABLE I. Comparing with the others method, the proposed method has the highest inter-region contrast, the lowest inter-region contrast and is faster. Furthermore, when observing the resulting images we can notice that the result given by the proposed method is the best one. The C-V's method based on global region information does not detect the entire object. The Li's and Chen's methods suffer from leakage specific to edge-based methods when the gradient on the boundaries is not well defined.

Figs. 3 and 4 show the experiment in noisy environment. In Fig. 3, the image is corrupted by a Gaussian noise with different values of the mean m and variance v . The proposed method is compared with the C-V's method which uses global statistics and therefore is robust against noise. The segmentation results demonstrate that the proposed method is more robust although it uses local statistics. In Fig. 4, the image is corrupted by the salt and pepper noise

with different density d . Here again the proposed model shows better performance than the global region based CV's model.

Fig. 5 demonstrates the performance of the proposed method for tumor segmentation in an MR image of head with presence of intensity heterogeneity. The executive times and the results of the objective evaluation are displayed by TABLE II. The Li's and Chen's methods suffer again from leakage since the boundaries are without edges. The C-V's method, based on global information, fails to detect the tumor. In opposition, our model shows its ability to segment object in presence of intensity heterogeneity, and faster than the others methods.

Fig. 6 shows the experimental results on a real world image, the executive times and the results of the objective evaluation are displayed by TABLE III. Here again, we can notice that the proposed method has the higher inter-region contrast and the lowest intra-region contrast; combining with the visual observation of the experimental results, we can conclude that the performances of the proposed algorithm are the best ones both in terms of speed and accuracy.

4. CONCLUSION

This work presents an image segmentation method based on the geometric formulation of active contours models. The local regions information and the Gaussian fuzzy membership function are used to define a new energy functional whose the minimization using the level set framework leads to an effective image segmentation in presence of intensity heterogeneity even in noisy environment. Contrary to local methods which are less sensitive to noise than global region methods, the proposed model is highly robust against noise. We use the highly parallelizable lattice Boltzmann method to solve the level set equation. As result, the method is fast when implemented using an NVIDIA GPU. Experimental results on a variety kinds of images have demonstrated subjectively and objectively the good performance of the proposed model in terms of efficiency, effectiveness, speed and robustness against noise.

Future work will be to handle the problem of memory complexity induced by LBM, and extend the introduced method to real-time volume images segmentation using a GPU cluster.

REFERENCES

- [1] S. Balla-Arabé and X. Gao, "Geometric Active Curve for Selective Entropy Optimization," *Elsevier Neurocomputing*, vol. 139, pp. 65-76, (2014).
- [2] S. Zhu and A. Yuille, "Region competition: unifying snakes, region growing, and Bayes/MDL for multiband image segmentation," *IEEE Transactions on Pattern Analysis and Machine Intelligence*, vol. 18, no. 9, pp. 884-900, (1996).
- [3] X.-B Gao, B. Wang, D. Tao and X. Li, "A relay level set method for automatic image segmentation," *IEEE Transactions on Cybernetics*, vol. 41, no. 2, pp. 518-525, (2011).
- [4] T. Chan, L. Vese, "Active contours without edges," *IEEE Transactions on Image Processing*, vol.10, no.2, pp. 266-277, (2001).
- [5] Y. Chen, Z. Yan and Y. Chu, "Cellular automata based level set method for image segmentation," *IEEE/ICME International Conference on Complex Medical Engineering*, Beijing, pp. 23-27, (2007).
- [6] Ye Zhao, "Lattice Boltzmann Based PDE Solver on the GPU," *The Visual Computer*, vol. 24, no. 5, pp. 323-333, Springer, (2007).

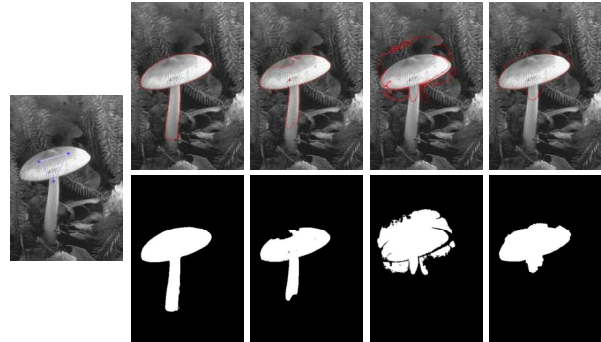


Fig. 2. Segmentation of natural image. First column: initial contour. Second column: result of the proposed method. Third column: result of the C-V's method. Fourth column: result of the Chen's method. Fifth column: result of the Li's method.

Table I. EXECUTIVE TIMES AND OBJECTIVE EVALUATION RESULTS.

Methods	Inter LN	Intra LN	Executive time (s)
Our method	0.2509	1.0400e-06	1.0565
C-V's method	0.1727	1.1889e-06	177.0856
Li's method	0.1785	2.9944e-06	34.3727
Chen's method	0.0973	5.1361e-06	19.0662

Image dimensions 481 X 321

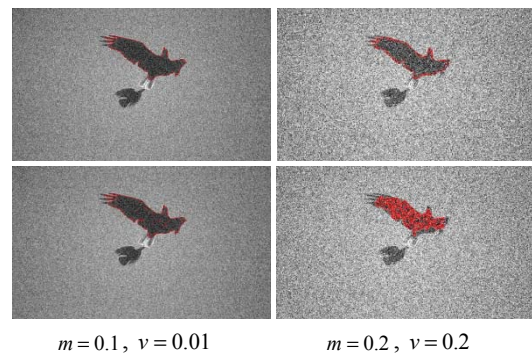


Fig. 3. Segmentation of an image corrupted by a Gaussian noise for different values of m and v . First row: result of the proposed method. Second row: result of the C-V's method.

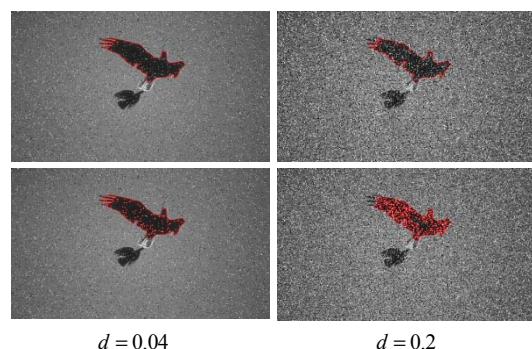


Fig. 4. Segmentation of an image corrupted by a Salt and pepper noise for different values of d . First row: result of the proposed method. Second row: result of the C-V's method.

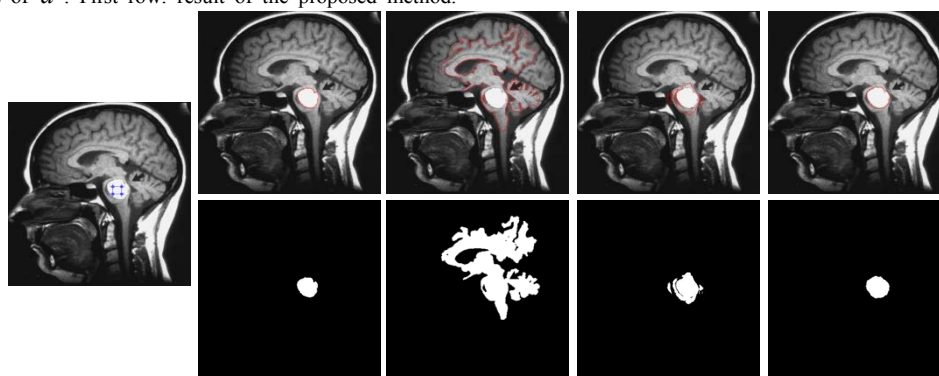


Fig. 5. Segmentation of a head tumor. First column: initial contour. Second column: result of the proposed method. Third column: result of the C-V's method. Fourth column: result of the Chen's method. Fifth column: result of the Li's method.

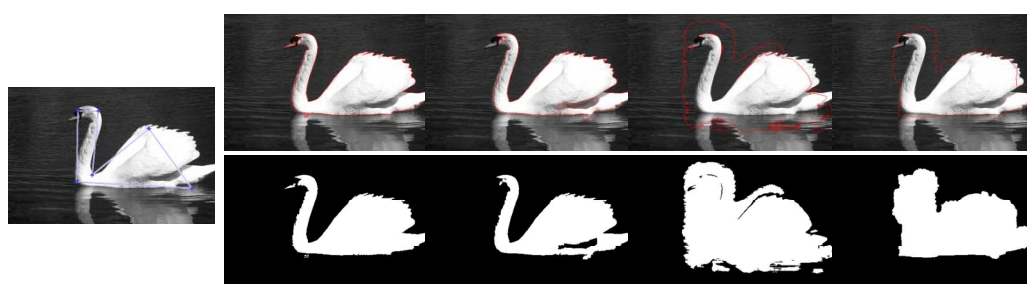


Fig. 6. Segmentation of a real world image. First column: initial contour. Second column: result of the proposed method. Third column: result of the C-V's method. Fourth column: result of the Chen's method. Fifth column: result of the Li's method.

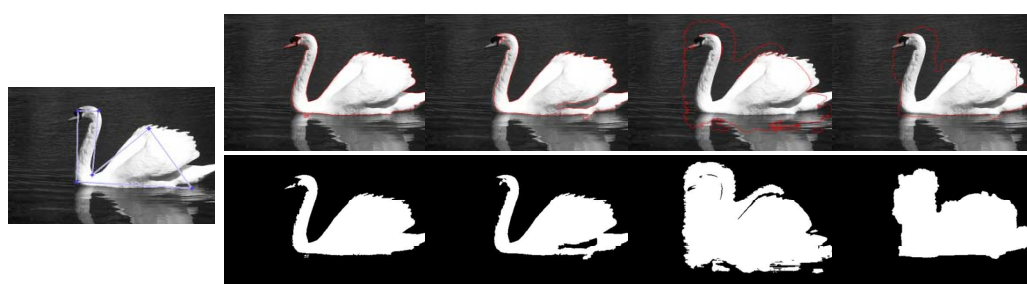


Table II. EXECUTIVE TIMES AND OBJECTIVE EVALUATION RESULTS.

Methods	Inter LN	Intra LN	Executive time(s)
Our method	0.1243	1.9696e-08	1.2625
C-V's method	0.0912	3.4791e-07	173.9056
Li's method	0.0712	6.4791e-07	21.2357
Chen's method	0.1033	2.7152e-06	10.5992

Image dimensions 431 X 400

Table III. EXECUTIVE TIMES AND OBJECTIVE EVALUATION RESULTS.

Methods	Inter LN	Intra LN	Executive time(s)
Our method	0.1489	1.4508e-07	1.1591
C-V's method	0.1463	7.1386e-07	104.8376
Li's method	0.1132	5.4287e-06	48.3095
Chen's method	0.1040	7.2446e-06	9.2420

Image dimensions 321 X 481

- [7] P. L. Bhatnager, E. P. Gross, and M. Krook, *Phys. Rev.* 94, 511 (1954).
- [8] G. Aubert and P. Kornprobst, "Mathematical Problems in Image Processing: Partial Differential Equations and the Calculus of variations," *Applied Mathematical Sciences*, vol. 147, Springer-Verlag, (2001).
- [9] S. Balla-Arabé, X.-B Gao, B. Wang, F. Yang and V. Brost, "Multi-Kernel Implicit Curve Evolution for Selected Texture Regions Segmentation in VHR Satellite Images," *IEEE Transactions on Geoscience and Remote Sensing*, vol. 52, no. 8, pp. 5183-5192, (2014).
- [10] J. G. Rosen, "The gradient projection method for nonlinear programming, II, Non-linear constraints," *J. SIAM*, vol.9, pp. 514-532, (1961).
- [11] C. Li, C. Xu, C. Gui and M.Fox, "Distance regularized level set evolution and its application to image segmenta-

tion," *IEEE Transactions on Image Processing*, vol. 19, no. 12, pp. 3243-3254, (2010).

- [12] S. Philipp-Foliguet and L. Guigues, "Evaluation of image segmentation: state of the art, new criteria and comparison," *traitement du signal*, vol. 23, no. 2, pp. 109-124, (2006).
- [13] G. Papandreou and P. Maragos, "Multigrid geometric active contour models," *IEEE Transactions on Image Processing*, vol. 16, no. 1, pp. 229-240, (2007).
- [14] S. Lankton and A. Tannenbaum, "Localizing Region-Based Active Contours," *IEEE Transactions on Image Processing*, vol. 17, no. 11, pp. 2029-2039, (2008).
- [15] N. Paragios and R. Deriche, "Geodesic active regions: A new framework to deal with frame partition problems in computer vision," *International Journal of Computer Vision*, vol. 46, no. 3, pp. 223-247, (2002).
- [16] S. Chapman and T.G. Cowling, *The Mathematical Theory of Non-Uniform Gases: An account of the kinetic Theory of Viscosity, Thermal Conduction and Diffusion in Gases*, Cambridge University Press, Cambridge, (1990).
- [17] S. Balla-Arabé, X. Gao and B. Wang, "A Fast and Robust Level Set Method for Image Segmentation Using Fuzzy Clustering and Lattice Boltzmann Method," *IEEE Transactions on Cybernetics*, vol. 43, no. 3, pp. 910-920, (2013).
- [18] S. Balla-Arabé and X. Gao, "Image multi-thresholding by combining the lattice Boltzmann model and a localized level set algorithm," *Elsevier Neurocomputing*, vol. 93, pp. 106-114, (2012).